



Fabrication of a Sensitive Biosensing System for Cu²⁺ ion Detection by Gold-Decorated Graphene Oxide Functionalized with Gly-Gly-His

Farnoosh Ostadakbari¹ · Fatemeh Yazdian² · Hamid Rashedi¹ · Amirhossein Ghaemi² · Bibi Fatemeh Haghirosadat³ · Marzieh Azizi⁴

Received: 11 May 2021 / Accepted: 31 August 2021 / Published online: 3 October 2021

© The Author(s), under exclusive licence to Springer Science+Business Media, LLC, part of Springer Nature 2021

Abstract

Incorporation of nanomaterials and nanostructures into sensors causes remarkable advances in device operation due to sensitivity, selectivity, multiplexed detection capability, and portability. In this study, a nanographene sensor coated with gold nanoparticles and tripeptide Gly–Gly–His was designed for Cu²⁺ ion detection at low concentrations. Graphene oxide synthesized by the modified Hummer's method and analyzed by UV–Vis spectrometry, x-ray diffraction (XRD), and transmission electron microscopy (TEM). The optimum conditions based on the maximum gold loading were evaluated 71 min for incubation time and 1 for HAuCl₄/HEPES concentration ratio. Gold-coating on graphene oxide was approved by TEM, UV–vis spectrometry, XRD, and FTIR. The EDC/Sulfo-NHS method was used to stabilize Gly-Gly-His to graphene oxide-gold, which has a high affinity toward Cu. The performance mechanism of this nanosystem was based on the localized surface plasmon resonance (LSPR) property of gold nanoparticles. The sensor was extremely selective and sensitive to Cu²⁺ with the detection limit of 8.83 nM without cross-binding to other metal ions. The response time was evaluated about 9 min. The GO-Au-GGH biosensor was also very stable and easily reused, which further confirms it as an efficient and sensitive Cu²⁺ ion detection device.

✉ Fatemeh Yazdian
yazdian@ut.ac.ir

✉ Hamid Rashedi
hrashedi@ut.ac.ir

Farnoosh Ostadakbari
farnoosh.oo@ut.ac.ir

Amirhossein Ghaemi
amirhosseinghaemi93@ut.ac.ir

Bibi Fatemeh Haghirosadat
fhaghirosadat@gmail.com

Marzieh Azizi
mar_azizi81@alumni.ut.ac.ir

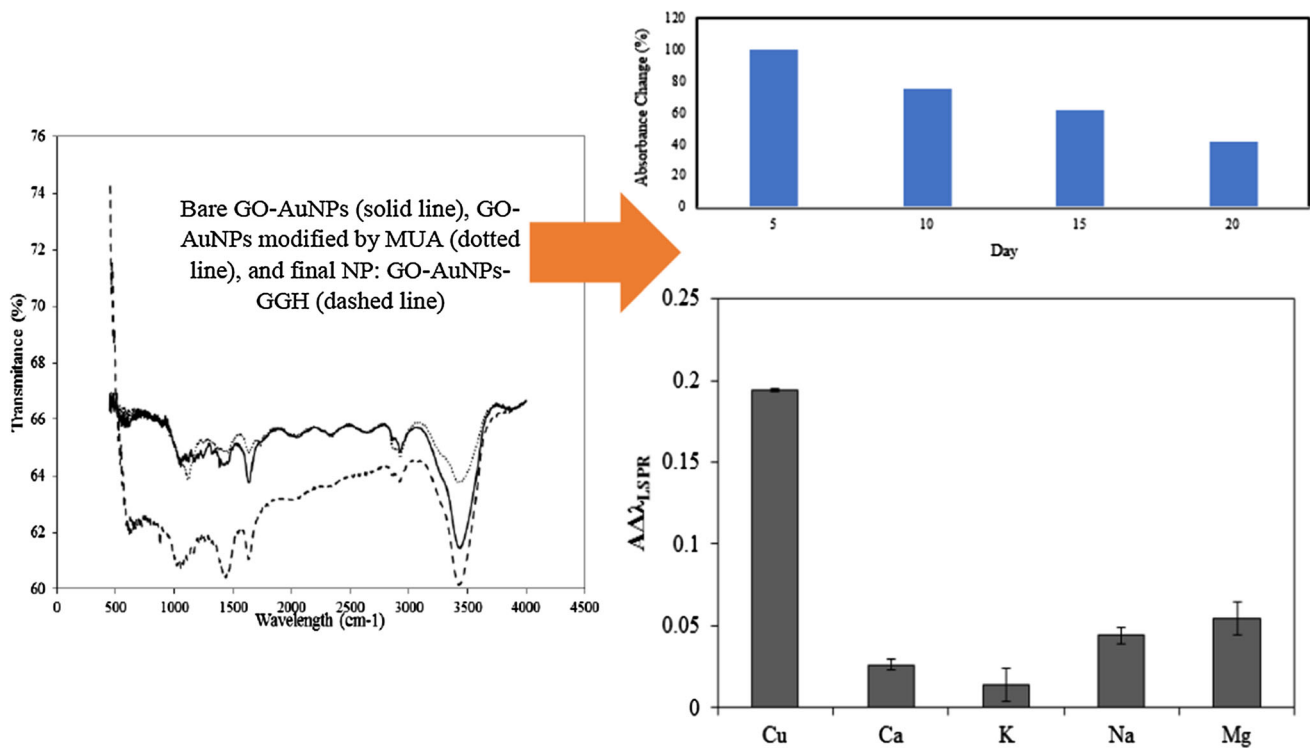
¹ School of Chemical Engineering, College of Engineering, University of Tehran, Tehran, Iran

² Department of Life Science Engineering, Faculty of New Science and Technologies, University of Tehran, Tehran, Iran

³ Department of Clinical Biochemistry, School of Medicine, Shahid Sadoughi University of Medical Sciences, Yazd, Iran

⁴ Institute of Biochemistry and Biophysics, University of Tehran, Tehran, Iran

Graphic Abstract



Keywords Copper sensing · Graphene nanostructures · Localized surface plasmon resonance (LSPR) · Nano-bio systems

Introduction

Heavy metals are not biodegradable and accumulate in the environment for a long time [1]. Accumulation of these metals leads to a severe problem for the health of living creatures, especially humans [2, 3]. The primary cause of the toxicity of these metals is the formation of a bond with the thiol group of proteins, which changes their structure [4]. The removal of these ions is essential not only because of their toxicity but also for reusing them in industries [5]. As a heavy metal, copper is a vital element for the human body and is a key factor in biological processes. However, the excess of Cu²⁺ may damage kidney and liver or cause gastrointestinal distress and neurodegenerative diseases. To avoid these problems, it is essential to detect Cu²⁺ ions [3].

There are various methods to detect heavy metal ions based on their range of concentration in the environment. For example, Spectroscopy has been used to identify heavy metals [6]. With remarkable achievements in nanotechnology and technology-based bioscience, biosensors are already being used to detect such ions. Biosensors are sensitive, specific, economical, and portable methods for ion detection [7]. Graphene-based materials have been

studied in bioengineering for high biocompatibility, low toxicity, high functionalization ability, and stable 2-D structure [8]. Between graphene-based materials, graphene oxide is the key material in developing carbon nanomaterials [9]. Liu et al. [10] suggested GO-modified Ag–In–Zn–S quantum dots in a fluorescent probe for Cu²⁺ ion detection. The proposed biosensor showed a selective and short-time response (1 min) in the range of 0–850 μM. In another study, a fluorescent probe for Cu²⁺ determination based on the fluorescence quenching of glyphosate-functionalized quantum dots was proposed by Liu et al. [11]. A limit detection of 1.3×10^{-3} μg/mL and pH of 6.8 was reported using the biosensor. They showed that surface ligands affect the fluorescence response of quantum dots to the ions and are, therefore, key factors of metallic ion selectivity.

In the current paper, a novel detection method for copper ions by incorporating the localized surface plasmon resonance (LSPR) property of gold NPs is introduced. Previous studies have found that the intensity and number of the SPR peaks are strongly influenced by environmental properties such as the refractive index [12]. In this work, an electrochemical graphene oxide sensor was decorated by

gold nanoparticles (AuNP) and functionalized with Gly-Gly-His (GGH) tripeptide. Copper ions induce the structure change in GGH, and SPR responds to refractive index changes with the affinity of a sensing surface. GGH operates as a copper ion receptor on the sensing surface because of peptides that have highly selective metal-binding properties. Next, the optimization of the synthesis of GO-AuNP hybrids was approved by TEM, XRD, and FTIR. The optimum conditions (the different molar ratios of HAuCl₄/HEPES and reaction times) based on maximum gold loading were evaluated. The response time, stability, selectivity, and sensitivity of the sensor were studied in detail. Results showed that the GO-Au-GGH sensor showed a higher affinity towards Cu²⁺ ions than the other ions.

Experimental

Materials

Chloroauric acid (HAuCl₄), potassium permanganate (KMnO₄), sodium hydroxide (NaOH), hydrogen chloride (HCl), sodium nitrate (NaNO₃), sulfuric acid (H₂SO₄), ethanol (C₂H₆O) were purchased from Merck. Gly-Gly-His, 4-(2-hydroxyethyl)-1-piperazineethanesulfonic acid (HEPES), 11-Mercaptoundecanoic acid, *N*-(3-Dimethylaminopropyl)-*N*-ethyl carbodiimide hydrochloride (EDC), *N*-Hydroxysuccinimide (NHS), Copper(II) sulfate (CuSO₄), were obtained from Sigma-Aldrich. pH was adjusted using either NaOH or HCl solutions. All the solutions were prepared with distilled water.

Synthesis of GO-AuNP and Optimization

The HAuCl₄ solution (0.1 M) was prepared in distilled water and stored in a refrigerator for further usage (at 4 °C).

GO was prepared using the modified Hummer's method [13]. 20 mg of prepared GO sheets were added to 20 ml deionized water. The solution was under bath sonication for 30 min; then, it was ultra-sonicated for 5 min. The product was a light brown homogeneous GO solution with a concentration of 1 mg/ml.

0.5 μL of GO solution (1 g/L) was mixed with HEPES solution (0.05, 0.1, 0.15 M) and its pH adjusted to 7.4 at room temperature. The mixture was ultra-sonicated for 5 min. HEPES has the piperazine ring, which consequently results in the formation of nitrogen-centered free radicals. Hence, HEPES synthesizes AuNPs as a reducing and shape-directing agent [14]. It can also manage the subsequent growth of gold NPs [15]. 0.2 μL of HAuCl₄ (0.1 M) was added to the mixed solution. During the experiment,

the sample was kept away from light and the pH was adjusted to 7.4.

To remove HEPES and any excess gold NPs, GO-Au hybrids were centrifuged at 5000 rpm for 10 min. The supernatant was eliminated and the same amount of water was replaced and centrifuged again. In order to optimize the production, two important parameters, namely the different molar (or concentration) ratios of HAuCl₄/HEPES (0.1/0.05, 0.1/0.1, and 0.1/0.15) and reaction times (30 min, 60 min, and 90 min) were tested. The experimental design was achieved using *Design-expert* software.

Based on experimental results, the optimized sample was synthesized and prepared for functionalization of the peptide.

Characterization of Samples

In order to study the surface structure and crystallinity of the prepared GO and GO-Au, TEM images and XRD were used. The characterizing functional groups of GO-Au was investigated by FTIR.

GGH Functionalization

EDC and NHS have chemically activated Gold NPs [16]. The preparation of AuNPs functionalized with high amounts of GGH peptide was catalyzed by EDC/NHS [17]. The amide bond between the AuNPs and GGH was improved using EDC. In parallel, NHS was added to the reaction mixture to enhance the efficacy of amide bonds and protect it from hydrolysis [18].

GO-Au was incubated in 1 mg/mL sulfo-NHS and 0.5 mg/mL MUA (11-Mercaptoundecanoic acid) buffer (pH 6.1). Following that, GGH peptide was mixed with a concentration of 0.8 g/mL and stabilized for 30 min. 1 g/mL EDC was then added to the mixture incubated (room temperature, 16 h). The GO-Au-GGH was centrifuged (14,000 rpm, 30 min) to eliminate the unfunctionalized peptides. GGH functionalization was studied by FTIR and UV spectrophotometry.

Cu²⁺ Ion Sensing

6-ml microtubes containing 60 μl biosensor solutions with different concentrations of copper were tested and read after two minutes by LSPR absorption spectrophotometry at a wavelength of 300–900 nm. All experiments were repeated three times.

Calibration Curve

1 μL standard copper solution with a concentration of 10 mg/ml was prepared in the micro-tubes, which contains

1 μL nano-bio sensing solution. After 2 min, it was measured by spectrophotometry at a wavelength of 300–900 nm. All experiments were repeated three times.

Selectivity of the LSPR Method

60 μL of Manganese was added to a micro-tube consisting of 1 μL of nano-biosensor, then incubated and read after two minutes by LSPR absorption spectrophotometry at a 300–900 nm wavelength. All experiments were repeated three times.

Response Time and Stability Measurement

To determine the response time, the response of LSPR was investigated through variations of absorption peak. 60 μL of copper solution with a concentration of 0.01 M was added to a micro-tube that contains 1 μL of nano-biosensor solution. Results were shown after 0,3,6,9, 20, and 25 min by LSPR absorption spectrophotometry at a wavelength of 300–900 nm.

To investigate the stability of biosensors, Results were read after first, 5th, 10th, and 20th by LSPR absorption spectrophotometry at the same wavelength.

Results and Discussion

Experimental Design

Response surface methodology (RSM) is a statistical method for optimizing complex processes. RSM needs the minimum number of experimentations and is an efficient and fast technique compared to other methods [19]. Central composite design (CCD) with a quadratic model was used to investigate the effects of independent variables incubation time and molar ratios of $\text{HAuCl}_4/\text{HEPES}$. The minimum and maximum values for the time were set at 30 and 90 min, and molar ratios of $\text{HAuCl}_4/\text{HEPES}$ were 0.1/0.05 and 0.1/0.15 as well. These two parameters play important roles in the gold loading mechanism. The experiments were repeated three times.

The statistical significance of the model was assessed by F values and analysis of variance (ANOVA), as presented in Table (in supplementary). The optimal conditions obtained using *Design Expert* software. The results revealed that the optimum conditions based on maximum gold loading are 71 min for incubation time and 1 for molar ratios of $\text{HAuCl}_4/\text{HEPES}$, respectively.

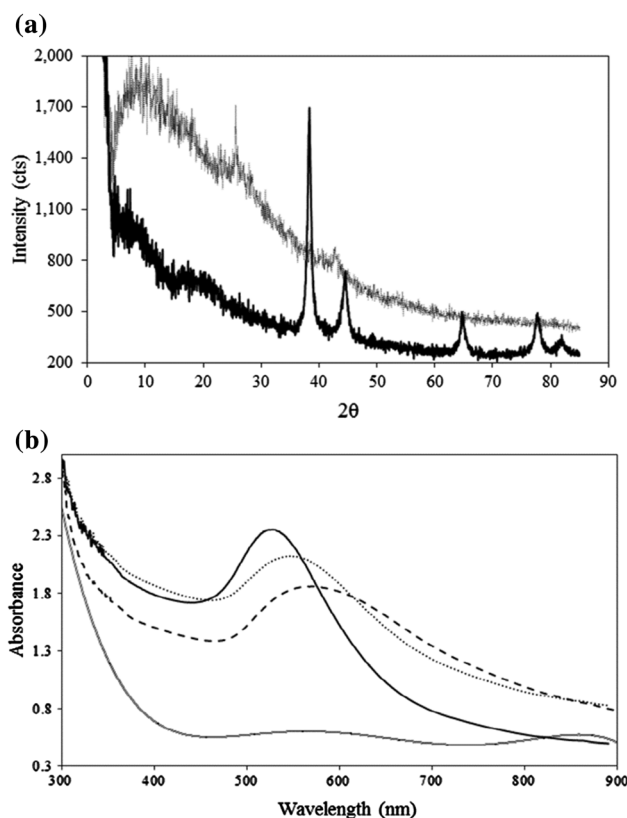


Fig. 1 a XRD pattern of GO–AuNPs (black line), GO (gray line), b presents the UV–Vis spectra of the different stages of modification. Bare GO–AuNPs (solid line), GO–AuNPs modified by MUA (dotted line), GO–AuNPs–MUA activated by EDC/NHS (dashed line), GO–AuNPs–GGH (double solid line)

UV–Vis Absorption Spectroscopy

The first step in validating GO–AuNPs formation was done using UV–Vis spectroscopy equipped with *Cary Win UV software*. UV–Vis spectra of GO–AuNPs and GO show a sharp peak at 537 nm in the GO–AuNPs spectrum that does not exist in the GO spectrum (supplementary). This peak verifies the formation of AuNPs on GO from HAuCl_4 . The peak height directly correlates with the content of AuNPs loaded onto GO in that the higher the peak height, the more AuNPs were loaded onto GO. Ting et al. [20] synthesized graphene quantum dots conjugated with gold NPs as an electrochemical sensor for Hg^{2+} and Cu^{2+} detection. They achieved a peak of 533 nm for GO–Au, which confirms our result.

Characterization of Samples

FTIR was done to determine the functional groups in GO–AuNPs. In the FTIR spectrum (in supplementary) of GO–AuNPs, apart from functional groups reported by other studies on GO, one peak was observed at 649 cm^{-1} , which

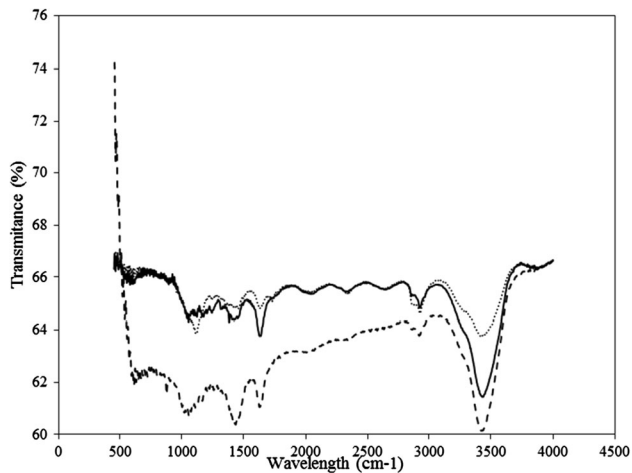


Fig. 2 FTIR spectra of different stages of modification. Bare GO-AuNPs (solid line), GO-AuNPs modified by MUA (dotted line), and final NP: GO-AuNPs-GGH (dashed line)

was related to the Au–O–Au vibrational bond. Saini et al. [21] also reported Au–O–Au peak transcription at 655 cm⁻¹. It was also considered that the peak intensity at 2923 and 2853 cm⁻¹ (–CH₂) and 1741 cm⁻¹ (C = O bond) decreased, which may be due to the attachment of gold NPs onto GO. The results are similar to those found by Aravind et al. [22] and Kim et al. [23], who worked on the electrochemical sensors of AuNP-modified graphene composites to detect lead and cholesterol, respectively.

The TEM image of GO and GO-AuNPs is in supplementary. The image represents the fairly uniform distribution of gold NPs on the surface of GO, which is important in the hybrid structure of GO and AuNPs. Aravind et al. [22] observed that gold nanostructures are accumulated in some zones while analyzing their synthesized AuNP-graphene biosensor.

XRD pattern was used to characterize the optimum formation of GO-AuNPs shown in Fig. 1a. The pattern of synthesized GO dispersion seen in the figure can be considered as confirmation of the loading of gold on the GO surface. As shown in Fig. 1a, GO has two peaks at 2θ of 9.31° and 25.56°. Luo et al. [24] obtained peaks for GO similar to the obtained peaks in this study. Related peaks to GO-AuNPs are as follows: 38.3° (111), 44.4° (200), 64.7° (220), 77.6° (311), and 81.7° (222), which confirm the formation of gold NPs on graphene according to the Gold Standard (JCPDS 89–3697).

GGH Functionalization

In Fig. 1b, the absorption diagram of different gold NPs is shown in four stages. For GO-AuNPs, the absorption peak of LSPR is observed at 530 nm (Fig. 1b solid line), whereas the absorption peak for the gold NP changed

via MUA shifts to 550 nm (Fig. 1b dotted line). This red-shift shows that the reaction between gold and sulfur causes the adsorption of alkanethiol molecules on the GO–Au surface. Furthermore, the formation of single-layer alkanethiol layers around the gold NP has led to a change in the absorption spectrum.

Activation by EDC/NHS was verified via the reduction of LSPR absorption peak at 550 nm (Fig. 1b dashed line), which showed surface changes on a metal NP. This modification causes accumulation and binding. The changes in the diagram confirmed the esterification of the terminal carboxyl groups in the NHS, which eliminated carboxylic ionization and neutralized the surface NPs.

Figure 2 displays the comparison of FTIR diagrams of GO–AuNPs, GO–AuNPs modified by MUA and GO–AuNPs–GGH. The peak is appearing at 1467 cm⁻¹ related to the C–H₃ bond. Crooks et al. [25] observed peaks at 2934, 2979, and 1467 cm⁻¹ for the C–H₃ bond. The FTIR analysis confirms the binding of the peptide to the GO–Au. As shown in Fig. 2, the peak related to the C–H₃ bond dropped to 1400 cm⁻¹ and, this confirms the peptide loading on GO–Au.

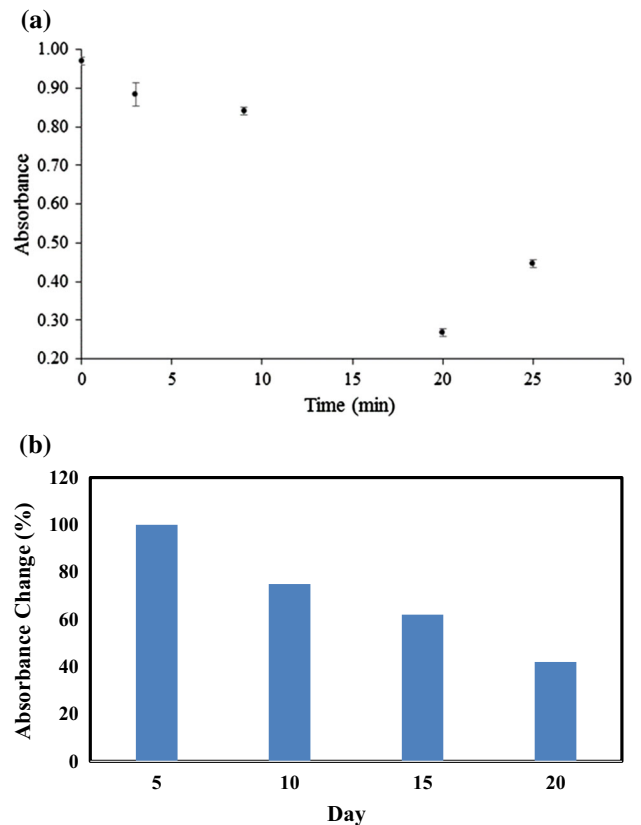


Fig. 3 **a** The biosensor response time (absorbance changes) versus time (minutes) at 0.1 μM of copper concentration, **b** biosensor performance (absorbance changes in %) versus time (days) at a copper concentration of 0.1 μM

Table 1 Comparison of other studies on Cu²⁺ ion detection

Author/year	Sensor	Response time (min)
Chen et al.[27]/2009	Rhodamine B hydroxylamide	120
Muthuraj et al.[28]/2014	Indole-3-carboxaldehyde functionalized fluorescein hydrazine	–
Pal et al.[29]/2015	Schiff base derived from rhodamine hydrazide and cinnamaldehyde	0.083–0.16
Tang et al.[30]/2016	Naphthalimide- rhodamine dyad	1 >
Chen et al.[31]/2017	Gold nanocluster	15
Huang et al.[32]/2017	Meso-tetra(4-sulfonatophenyl)porphine dihydrochlorid assembled SiO ₂ -encapsulated β-NaYF ₄ :Yb,Er,Gd nanorods	0.16
Wang et al.[33]/2017	Hydrazone bearing 1,8-naphthalimide & pyrrole moieties	5
Kim et al.[34]/2017	Aniline- functionalized silica NPs	3
Bao et al.[35]/2018	1,8-naphthalimide- based derivative	1 >
In this study	GO–Au–GGH	9

Detection of Copper

As mentioned in the previous sections, the LSPR wavelength is sensitive to the change in the refractive index. Hence, changes in the refractive index in the adjacent NP environment will change the LSPR wavelength [26].

The response time of the LSPR absorption peak variations of copper ions with different concentrations is shown in supplementary. As can be seen, the copper ion causes changes in the LSPR absorption peak. Changes in the structure of the protein were observed to result in changes in the LSPR peak absorption. Decreasing copper ion concentration increased the peak difference.

Calibration Curve

The calibration curve of the biosensor is shown in supplementary. There is a linear relationship between changes in the absorption peak of the LSPR and the concentration

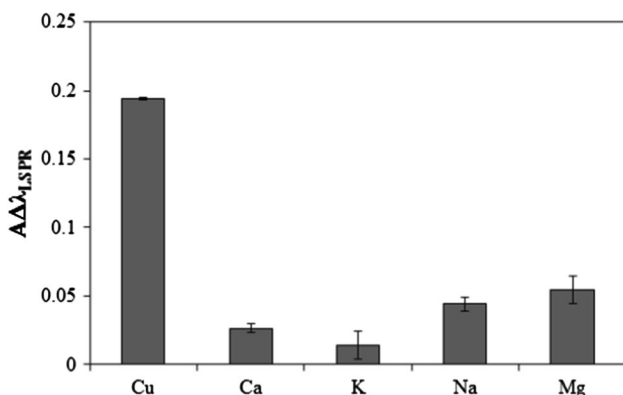


Fig. 4 Specificity of the biosensor response versus copper ion and the other ions in water at 10 nM of ions

of copper. A linear range of 0.01 nM–0.1 μM was observed. The sensitivity of the biosensor can be calculated by using the slope of the line diagram of changes in the absorption peak of the LSPR and the concentration of the copper ion. The sensitivity of the biosensor to the copper ion was calculated as 0.08 nm/μM. The detection limit of an individual analytical procedure is the lowest amount of analyte in a sample which can be detected but not necessarily quantitated as an exact value. Several approaches for determining the detection limit are possible. The limit of detection (LOD) was calculated based on the following equation:

$$\text{LOD} = \frac{3 \times \text{standard deviation of low concentration}}{\text{slope of the calibration line}}$$

By this method, LOD was obtained as 0.00883 μM or 8.83 nM.

Response Time and Stability

In order to examine biosensor response, it was alternately exposed to a certain amount of copper ions. Figure 3a shows the time response of the LSPR absorption. As you can see, after nine minutes, the difference between peaks increased and reveal that the response time of GO_Au_GGH is 9 min. The response time of the biosensor compared with other Cu²⁺ ion detection studies in Table 1.

For stability purposes, biosensor response was tested at a concentration of 60 μM in a 20-day interval, as measured by the changes in LSPR peak absorption to copper ion. As seen in Fig. 3b, after a 20-day period at refrigerator temperature (4 °C) [36], the biosensor response changed and decreased by 42%.

Table 1 comprise the results of Cu²⁺ ion detection researches in recent years. As it is obvious, GO–Au–GGH is a sensitive and accurate sensor.

Selectivity

Another critical parameter to be considered is biosensor specificity. For this purpose, the number of changes in the absorption peak of the LSPR sensor was evaluated in the form of the specific concentrations of various ions (K⁺, Na⁺, MN²⁺, Ca). The biosensor was seen to have good specificity to copper ion, as shown in Fig. 4.

Conclusions

In this study, GO was used as a suitable nanoclay for loading gold ions and GGH. Modified Hummer's method was used to synthesize GO, and characterized by XRD, UV–Vis spectrometry, and TEM. Next, Gold ion was coupled to the surface of GO and the process of bonding gold ions to GO surface optimized using different times and the concentration ratios of HEPES/graphene. An optimum sample was selected for ultraviolet absorption spectroscopy. Gold loading on GO was then discussed and confirmed using XRD, FTIR, and TEM images. GGH coupling was performed by the reaction between the amine and carboxyl groups and forming amide groups in the presence of EDC/sulfo-NHS. The loading of the peptide on nanohybrid was confirmed by FTIR and UV–Vis spectrometry.

The results demonstrate that the GO–Au–GGH biosensor is highly sensitive to Cu²⁺ and nearly insensitive to K⁺, Na⁺, MN²⁺, Ca²⁺ ions, with a detection limit of 8.83 nM. The response time was evaluated 9 min. The GO–Au–GGH biosensor was also very stable and easily reused, confirming it as an efficient and sensitive Cu²⁺ ion detection device.

Declarations

Conflict of interest The authors declare that they have no conflict of interest.

References

- Z. Xu, L. Zhong, and A. Zhang (2019). *IEEE Access* **7**, 163172–163179.
- M. Li, Z. Zhang, R. Li, J. J. Wang, and A. Ali (2016). *Int. J. Biol. Macromol.* **86**, 876–884.
- L. Dimple (2014). *Int. J. Environ. Res. Dev.* **4**, 8.
- Z. Xia, L. Baird, N. Zimmerman, and M. Yeager (2017). *Appl. Surf. Sci.* **416**, 565–573.
- I. M. Kenawy, M. A. H. Hafez, M. A. Ismail, and M. A. Hashem (2018). *Int. J. Biol. Macromol.* **107**, 1538–1549.
- G. L. Turdean (2011). *Int. J. Electrochem.* **2011**, 1–15.
- B. Janfada, F. Yazdian, G. Amoabediny, and M. Rahaie (2015). *Biotechnol. Appl. Biochem.* **62**, 349–356.
- M. Hashemi, A. Yadegari, G. Yazdanpanah, M. Omid, S. Jabbehdari, F. Haghirsadat, F. Yazdian, and L. Tayebi (2017). *Biotechnol. Appl. Biochem.* **64**, 433–442.
- S. Castrignano, F. Valetti, G. Gilardi, and S. J. Sadeghi (2016). *Biotechnol. Appl. Biochem.* **63**, 157–162.
- Y. Liu, M. Deng, X. Tang, T. Zhu, Z. Zang, X. Zeng, and S. Han (2016). *Sens. Actuat. B* **233**, 25–30.
- Z. Liu, S. Liu, P. Yin, and Y. He (2012). *Anal. Chim. Acta* **745**, 78–84.
- X. Fan, I. M. White, S. I. Shopova, H. Zhu, J. D. Suter, and Y. Sun (2008). *Anal. Chim. Acta* **620**, 8–26.
- W. S. Hummers and R. E. Offeman (1958). *J. Am. Chem. Soc.* **80**, 1339–1339.
- L. Hwang, C.-L. Chen, and N. L. Rosi (2011). *Chem. Commun.* **47**, 185–187.
- Q. Liu, L. Lai, H. Huang, J. Sun, T. Shang, Q. Zhou, and Z. Xu (2010). High-yield synthesis of branched gold nanocrystals by a sodium diphenylamine-4-sulfonate reduction process in polyethylene glycol aqueous solution. *Chin. J. Chem.* **28**, 537–542.
- S. Schreier, G. Doungchawee, S. Chadsuthi, D. Triampo, and W. Triampo (2011). *Biologia* **66**, 8–17.
- D. Li, Q. He, Y. Cui, L. Duan, and J. Li (2007). *Biochem. Biophys. Res Commun.* **355**, 488–493.
- A. Kumar, H. Ma, X. Zhang, K. Huang, S. Jin, J. Liu, T. Wei, W. Cao, G. Zou, and X.-J. Liang (2012). *Biomaterials* **33**, 1180–1189.
- M. Kumar, G. Singh, S. K. Arya, J. S. Bhatti, and P. Sharma (2018). *Biocatal. Agric. Biotechnol.* **14**, 235–240.
- S. L. Ting, S. J. Ee, A. Ananthanarayanan, K. C. Leong, and P. Chen (2015). *Electrochim. Acta* **172**, 7–11.
- D. Saini, R. Chauhan, P. R. Solanki, and T. Basu (2012). *ISRN Nanotechnol.* **2012**, 12.
- S. S. J. Aravind, T. T. Baby, T. Arockiadoss, R. B. Rakhi, and S. Ramaprabhu (2011). *Thin Solid Films* **519**, 5667–5672.
- H.-U. Kim, H. Y. Kim, A. Kulkarni, C. Ahn, Y. Jin, Y. Kim, K.-N. Lee, M.-H. Lee, and T. Kim (2016). *Sci. Rep.* **6**, 34587.
- Y. Luo, F.-Y. Kong, C. Li, J.-J. Shi, W.-X. Lv, and W. Wang (2016). *Sens. Actuat. B* **234**, 625–632.
- R. M. Crooks, H. C. Yang, L. J. McEllistrem, R. C. Thomas, and A. J. Ricco (1997). *Faraday Discussions* **107**, 285–305.
- J. Homola, S. S. Yee, and G. Gauglitz (1999). *Sens. Actuat. B* **54**, 3–15.
- X. Chen, J. Jia, H. Ma, S. Wang, and X. Wang (2009). *Anal. Chim. Acta* **632**, 9–14.
- B. Muthuraj, R. Deshmukh, V. Trivedi, and P. K. Iyer (2014). *ACS Appl. Mater. Interfaces* **6**, 6562–6569.
- S. Pal, B. Sen, S. Lohar, M. Mukherjee, S. Banerjee, and P. Chattopadhyay (2015). *Dalton Trans.* **44**, 1761–1768.
- J. Tang, S. Ma, D. Zhang, Y. Liu, Y. Zhao, and Y. Ye (2016). *Sens. Actuat. B* **236**, 109–115.
- S. Chen, Y. Kuang, P. Zhang, Y. Huang, A. Wen, X. Zeng, R. Feng, H. Nie, X. Jiang, and Y. Long (2017). *Sens. Actuat. B* **253**, 283–291.
- X. Huang, L. Wang, X. Zhang, X. Yin, N. Bin, F. Zhong, Y. Liu, and Q. Cai (2017). *Sens. Actuat. B* **248**, 1–8.
- Y. Wang, P.-D. Mao, W.-N. Wu, X.-J. Mao, X.-L. Zhao, Z.-Q. Xu, Y.-C. Fan, and Z.-H. Xu (2017). *Sens. Actuat. B* **251**, 813–820.

34. D. B. Kim, J. M. Hong, and S.-K. Chang (2017). *Sens. Actuat. B* **252**, 537–543.
35. Z. Bao, C. Qin, J.-J. Wang, J. Sun, L. Dai, G. Chen, and F. Mei (2018). *Sens. Actuat. B* **265**, 234–241.
36. M. Pourmadadi, J. S. Shayeh, M. Omid, F. Yazdian, M. Alebouyeh, and L. Tayebi (2020). *Microchim. Acta* **186** (12), 787.

Publisher's Note Springer Nature remains neutral with regard to jurisdictional claims in published maps and institutional affiliations.